SLICE-3D: A three-dimensional conservative semi-Lagrangian scheme for transport problems

Mohamed Zerroukat

(Nigel wood & Andrew Staniforth)

Met Office, Exeter, UK

SRNWP-NT, Zagreb, 2006

Content

- SLICE-3D specifications
- Brief review of SLICE-1D & SLICE-2D
- SLICE-3D
- Test results
- Conclusions

SLICE-3D specifications

1. SLICE-3D is a conservative and computationally efficent semi-Lagrangian scheme for the transport of scalars.
2. SLICE-3D uses multiple sweeps of a one-dimensional remapping algorithm along Eulerian and Lagrangian directions. This cascade-type splitting, and flow-dependent, strategy reduces the splitting error compared to traditional fixed direction-based splitting.
3. SLICE-3D does not compute at any stage, or needs to know, about the complex geometry of irregular Lagrangian volumes. This constitute an andvantage by comparison to volume-based multi-dimensional remapping.
4. SLICE-3D uses a C-grid wind-density staggering arrangements.
5. SLICE-3D would work by taking the vertical as the first cascade direction. This is for following reasons:

   (a) since the grid spacing in the vertical is known and is the same at each timestep, a higher-order remapping scheme can be applied efficiently as various factors can be precomputed and stored

SLICE-3D specifications

(b) it is possible to impose exactly a global max/min that is non-zero since the cross-sectional area is known exactly.

6. Having cascaded in the vertical, we are left with N (the number of vertical levels) SLICE-2D problems in the (deformed) horizontal. SLICE-2D in turn is a series of horizontal sweeps of the same 1d-remapping algorithm.
7. All distances used SLICE-3D are 3D physical distances.
8. SLICE-3D computes some 3D and 2D interesctions. This overhead is wind (or deformed geometry) dependent and independent of scalars. Therefore, it is anticipated that this overhead will be relatively small when SLICE-3D is used for a large number of physical/chemical species.

SLICE-1D approach

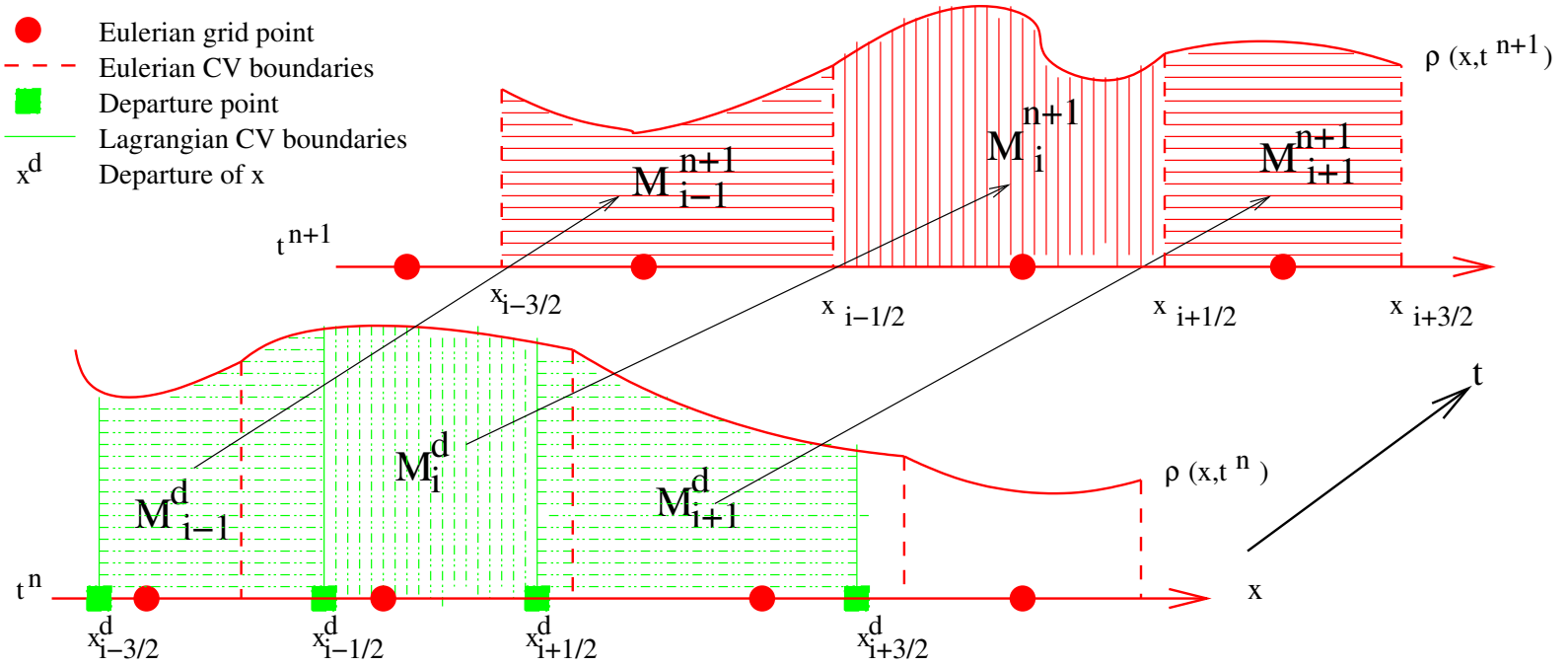

Reconstruction (PCM)

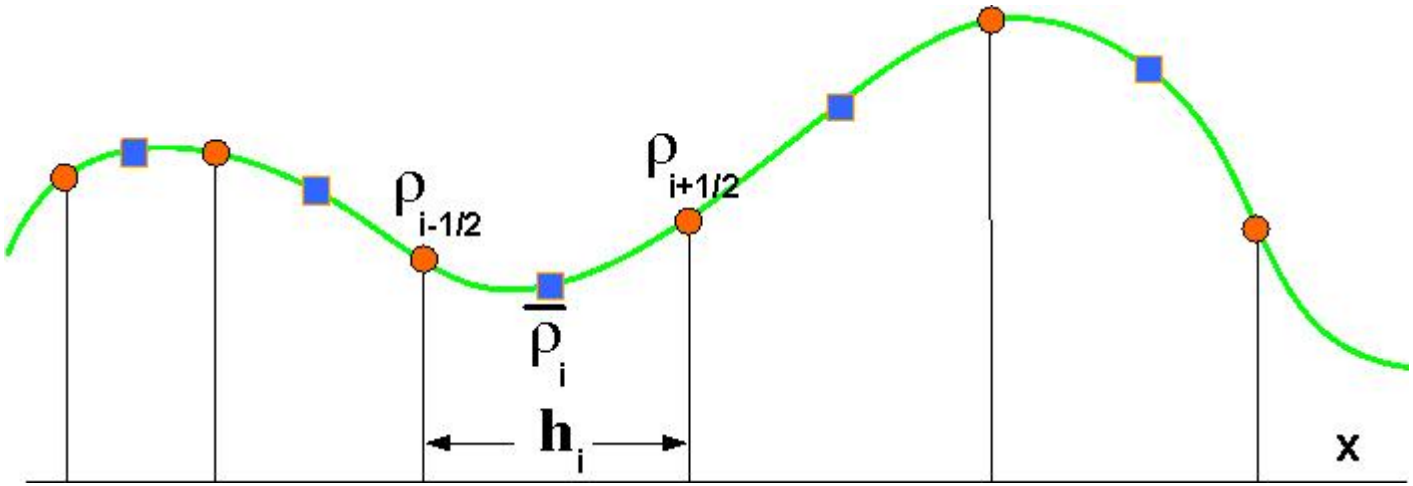

The Piecewise Cubic Method (*Zerroukat, Wood and Staniforth, Q. J. R. Meteo. Soc., 2002***)**

$$\rho_i(\xi) = a_i + b_i\xi + c_i\xi^2 + d_i\xi^3,\ \xi \in [0,1] \qquad (1)$$

that satisfies:

$$\overline{\rho}_i = \int_0^1 \rho_i(\xi)\, d\xi \ \ , \ \ \rho_i(0) = \rho_{i-1/2} \ \ , \ \ \rho_i(1) = \rho_{i+1/2} \ \ , \ \ \left.\frac{d\rho_i}{d\xi}\right|_{\xi=1/2} = \delta\rho_i \qquad (2)$$

Reconstruction (PCM)

where

$$\left.\begin{aligned} a_i &= \rho_{i-1/2}, \\ b_i &= -6\rho_{i-1/2} + 6\overline{\rho}_i - 2\delta\rho_i, \\ c_i &= 9\rho_{i-1/2} - 3\rho_{i+1/2} - 6\overline{\rho}_i + 6\delta\rho_i, \\ d_i &= -4\rho_{i-1/2} + 4\rho_{i+1/2} - 4\delta\rho_i. \end{aligned}\right\} \qquad (3)$$

Evaluation of the 3 unknown cubic parameters $\left\{\rho_{i-1/2}, \rho_{i+1/2}, \delta\rho_i\right\}$

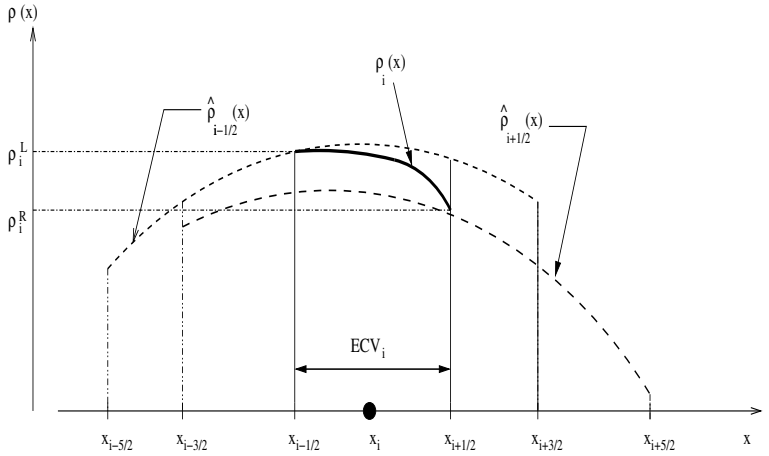

Reconstruction (PSM)

PCM + ($\delta\rho_i = \rho_{i+1/2} - \rho_{i-1/2}$) —> Parabola (Piecewise Parabolic Method (PPM) of Colella and Woodward, *J. Comput. Phys. 1984*):

$$\rho_i(\xi) = a_i + b_i\xi + c_i\xi^2,\ \xi \in [0,1] \tag{4}$$

that satisfies

$$\overline{\rho}_i = \int_0^1 \rho_i(\xi)\, d\xi \quad , \quad \rho_i(0) = \rho_{i-1/2} \quad , \quad \rho_i(1) = \rho_{i+1/2} \tag{5}$$

Parabolic Spline Method (PSM) (*Zerroukat, Wood and Staniforth, Int. J. Num. Meth. Fluids, 2006***)**

$$\frac{d\rho_i}{dx} = \left.\frac{d\rho_{i+1}}{dx}\right|_{x_{i+1/2}} \Rightarrow \frac{1}{h_i}\rho_{i-\frac{1}{2}} + 2\left(\frac{1}{h_i} + \frac{1}{h_{i+1}}\right)\rho_{i+\frac{1}{2}} + \frac{1}{h_{i+1}}\rho_{i+\frac{3}{2}} = 3\left(\frac{\overline{\rho}_i}{h_i} + \frac{\overline{\rho}_{i+1}}{h_{i+1}}\right) \tag{6}$$

PSM is more accurate than PPM but with a computational cost of only 60% of that of PPM

PSM (Monotonicity)

1. Non-monotonic behaviour at the grid scale

(a) The estimates $\{\rho_{i-1/2},\ i = 1, 2, ...\}$ at the cell boundaries are tested for undershoots and overshoots with respect to $\{\bar{\rho}_i,\ i = 1, 2, ...\}$

(b) The non-monotonic values are corrected (the closest ρ_i)

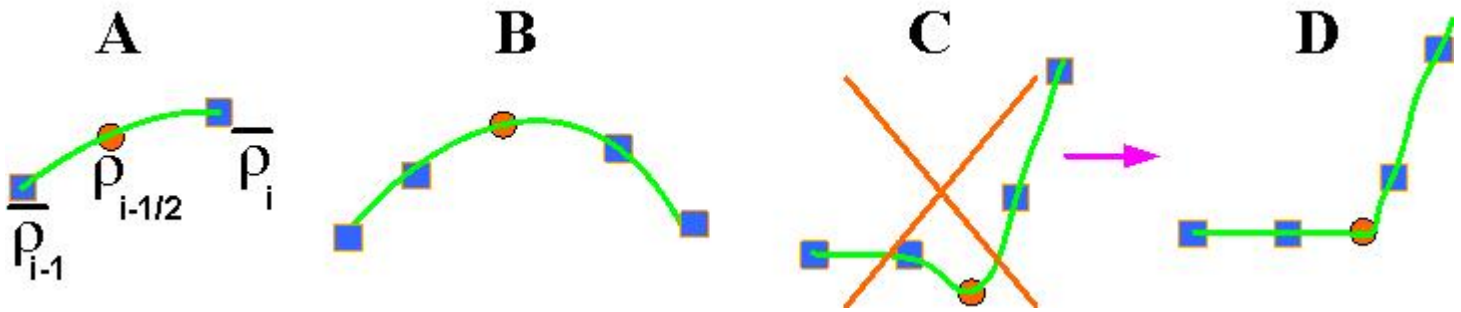

PSM (Monotonicity)

1. Non-monotonic behaviour at the sub-grid scales

(a) The parabola is tested for non-monotonic behaviour within the interval $\xi \in [0, 1]$

(b) The parabola is modified to the limiting case of monotonicity (discontinuities)

(c) If the limiting case is not possible $\Longrightarrow$ **piecewise constant profile**

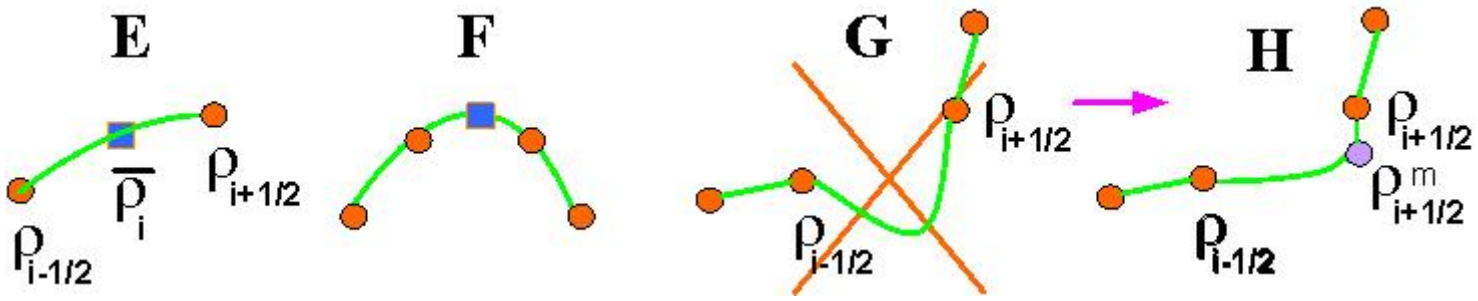

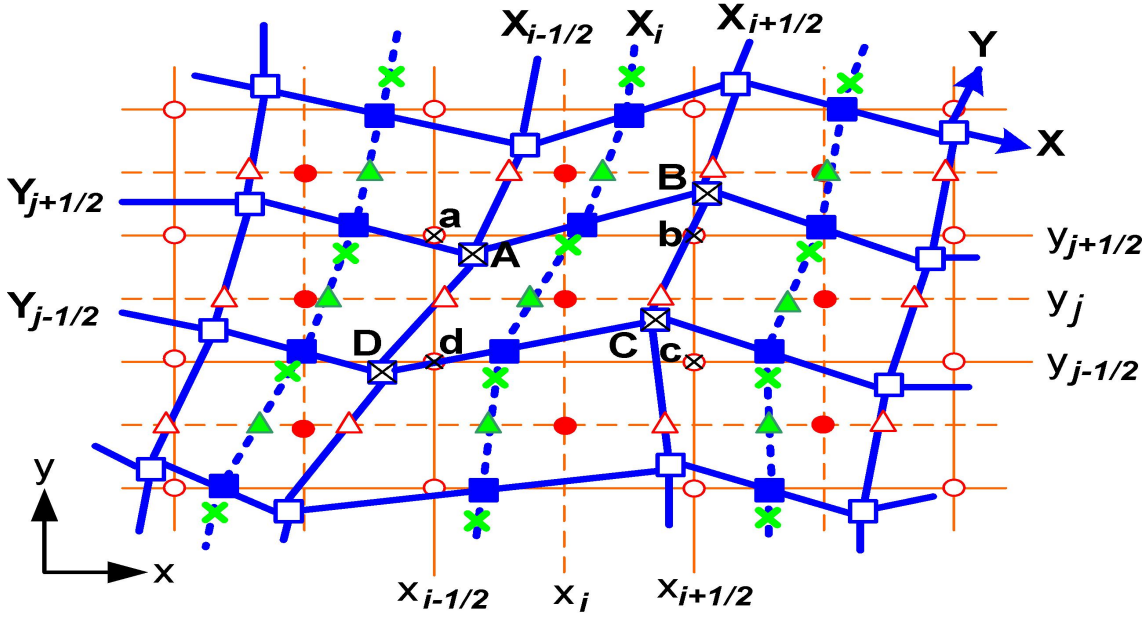

Figure 1: Superposition of Lagrangian and Eulerian grids away from poles.

SLICE-2D (polor cap region)

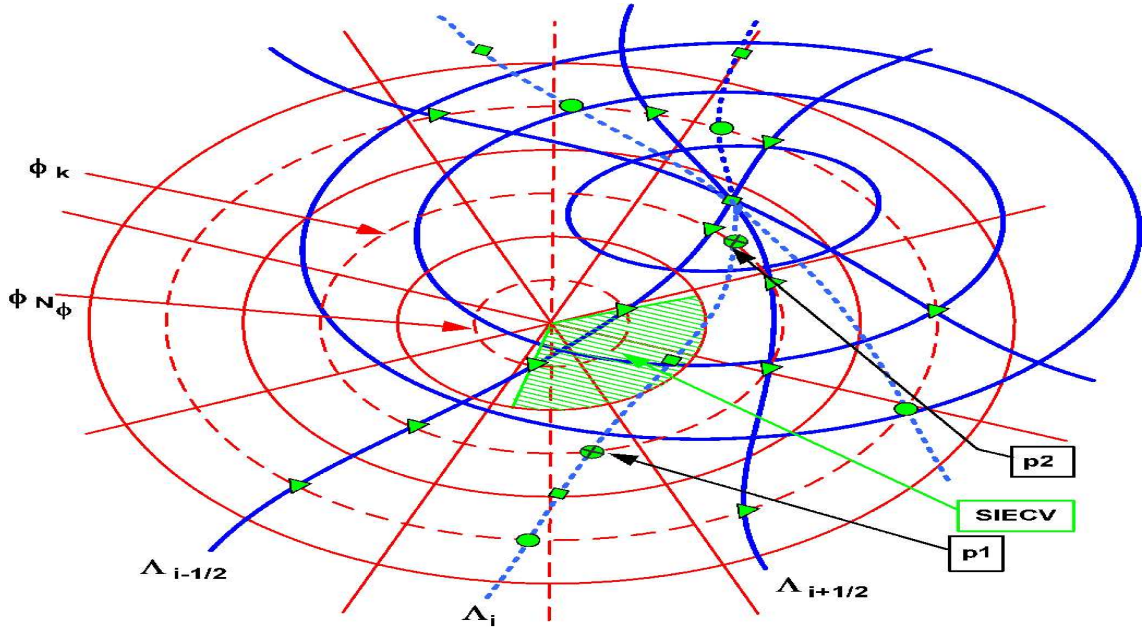

Figure 2: Superposition of Lagrangian and Eulerian grids in the vicinity of the north pole.

SLICE-2D

To take into account for the inaccuracy of the pivoting assumption for a region near the poles (polar cap), the density field is corrected (while maintaining mass conservation), using standard Semi-Lagrangian solution as a guide, i.e.,

$$\overline{\rho}_{i,j}^{n+1} = \begin{cases} \overline{\rho}_{i,j}^{c} = \dfrac{\sum_{l=k-1}^{N_\phi} \sum_{m=1}^{N_\lambda} \overline{\rho}_{l,m}^{*} EA_{l,m}}{\sum_{l=k-1}^{N_\phi} \sum_{m=1}^{N_\lambda} \rho_{l,m}^{SSL} EA_{l,m}} \rho_{i,j}^{SSL}, & \textbf{for} \quad i = 1, ..., N_\lambda; \quad j = k-1, ..., N_\phi \\ \overline{\rho}_{i,j}^{*}, & \textbf{otherwise} \end{cases}, \qquad (7)$$

SLICE-3D remapping

1. **Given the Eulerian masses $m_{i,j,k}$ for the spherical Eulerian Control-Volumes ($ECV_{i,j,k}$). $ECV_{i,j,k}$ is delimited by $\lambda_{i-1/2}$ and $\lambda_{i+1/2}$ in the λ-direction; by $\phi_{j-1/2}$ and $\phi_{j+1/2}$in the ϕ-direction; and by $r_{k-1/2}$ and $r_{k+1/2}$in the r-direction ($Volume = 1/3\ \delta r^3\ \delta\lambda\ \delta(\sin\phi)$)**
2. **The union of all the grid-points $(\lambda_{\forall i-1/2}, \phi_{\forall j-1/2}, r_{k-1/2})$ for a constant $k-1/2$, forms a discrete regular spherical Eulerian Shell (ES) $k-1/2$ ($k=1/2$ (surface) and $k=K+1/2$ (top surface)); The union of all the grid points $(\lambda^d_{\forall i-1/2,\forall j-1/2,k-1/2}, \phi^d_{\forall i-1/2,\forall j-1/2,k-1/2}, r^d_{\forall i-1/2,\forall j-1/2,k-1/2})$ form a discrete deformed closed (irregular) Lagrangian Shell (LS) $k-1/2$. (ES + wind) —> LS.**
3. **Each LS $k-1/2$ (including bottom and top surfaces) intersects each column (i,j) at a hight $r'_{k-1/2}$, $k=1,...,K+1$ (vertical intersection computation).**
4. **Given the set of masses $\{m_{i,j,k}, k=1,...,K\}$, for each column (i,j), perform a SLICE-1D to compute the intermediate masses$\{m'_{i,j,k}, k=1,...,K\}$ of the Intermediate Vertical Control Volume ($IVCV_{ij,k}$). $IVCV_{ij,k}$ is delimited by $\lambda_{i-1/2}$ and $\lambda_{i+1/2}$ in the λ-direction; by $\phi_{j-1/2}$ and $\phi_{j+1/2}$in the ϕ-direction; and by $r'_{k-1/2}$ and $r'_{k+1/2}$in the r-direction.**
5. **Given the intermediate masses $\{m'_{i,j,k},\ i=1,...,N;\ j=1,...,M\}$of a spherical annuli $k=1,...,K$ (volume between two LS's $k-1/2$ and $k+1/2$), use SLICE-2D to remap mass from the IVCVs to its final Lagrangian CVs (LCVs).**

SLICE-3D (cont.)

Lagrangian(blue) Eulerian (red) grids & vertical intersections (+megenta)(ORIGINAL POLAR)

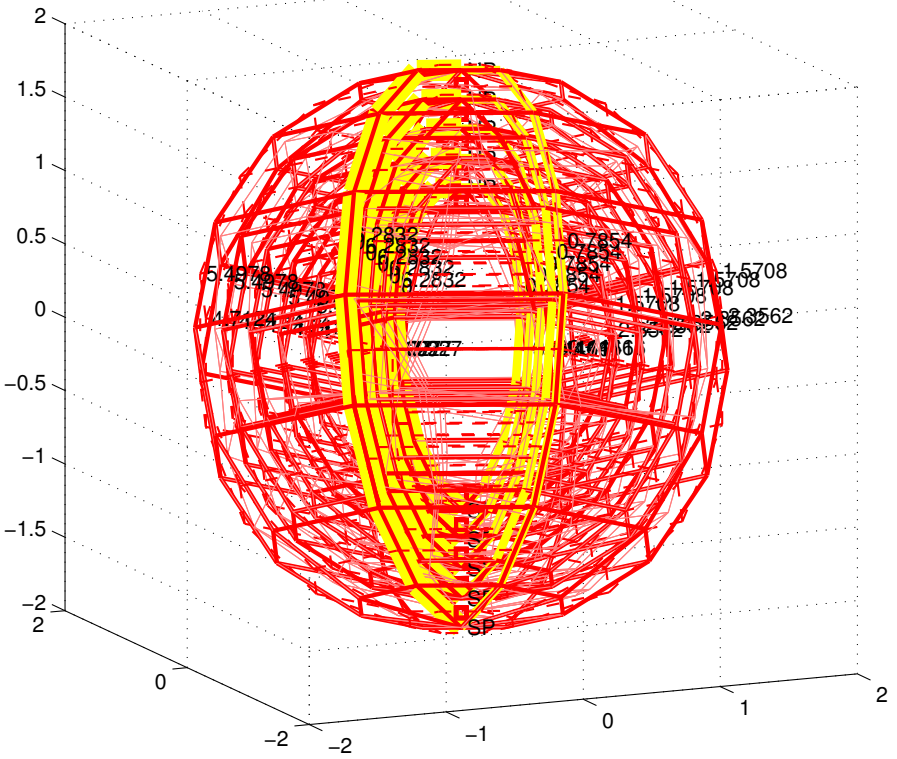

Lagrangian(blue) Eulerian (red) grids & vertical intersections (+megenta)(ORIGINAL POLAR)

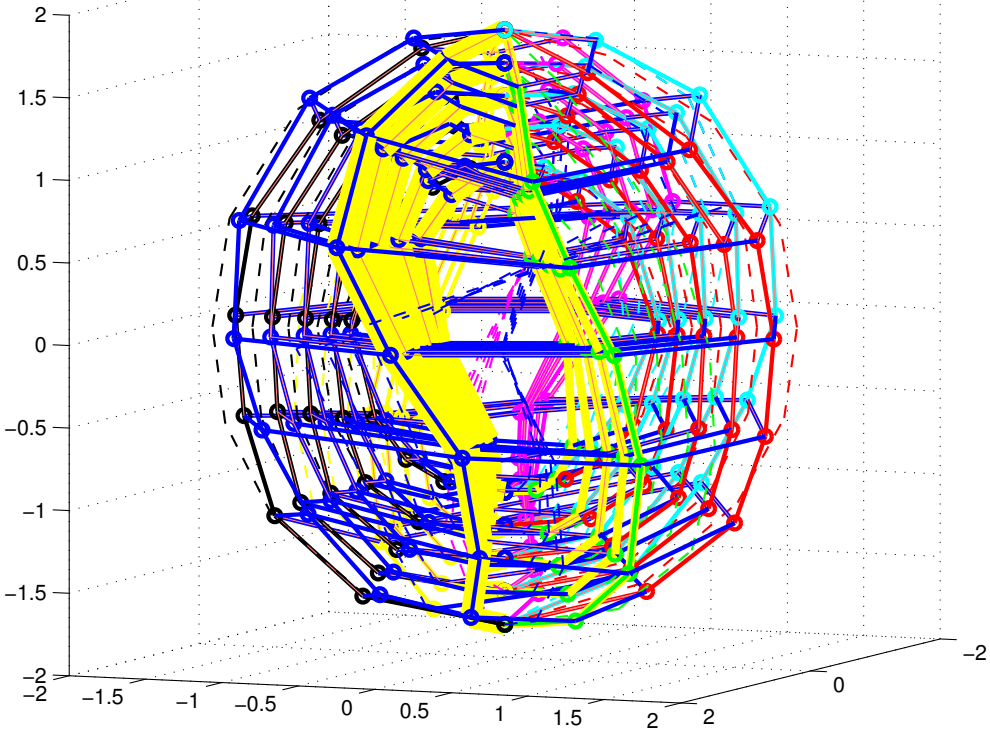

SLICE-3D (cont.)

Lagrangian(blue) Eulerian (red) grids & vertical intersections (+megenta)(MODIFIED CARTESIA

Lagrangian(blue) Eulerian (red) grids & vertical intersections (+megenta)(MODIFIED CARTESIAN)

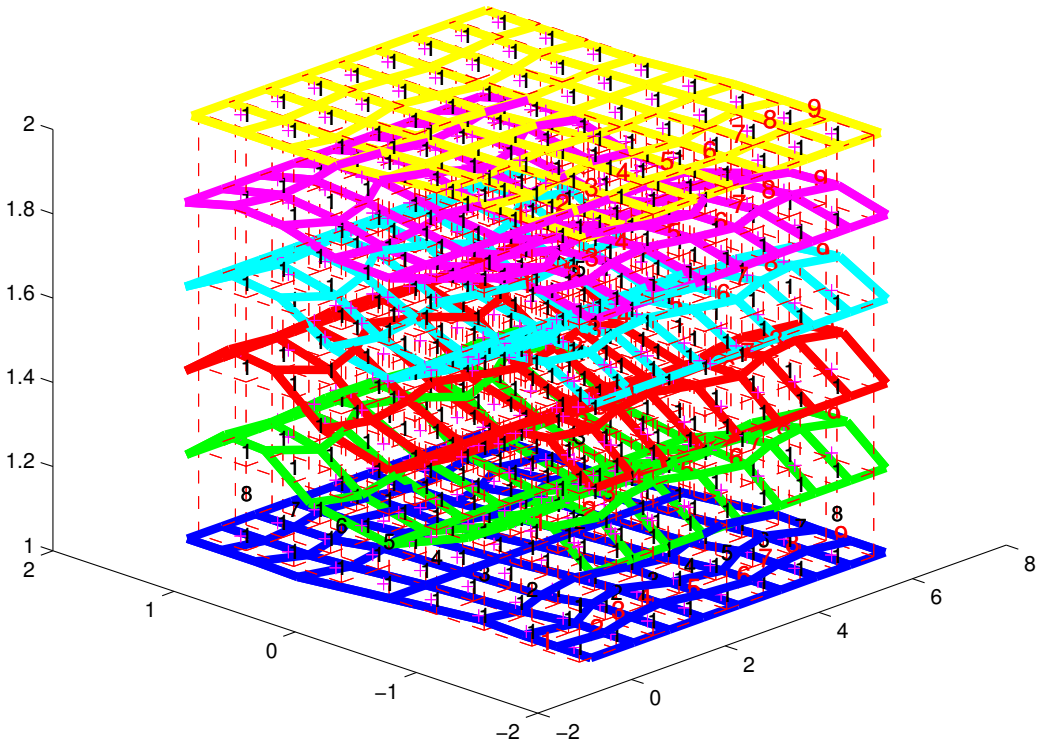

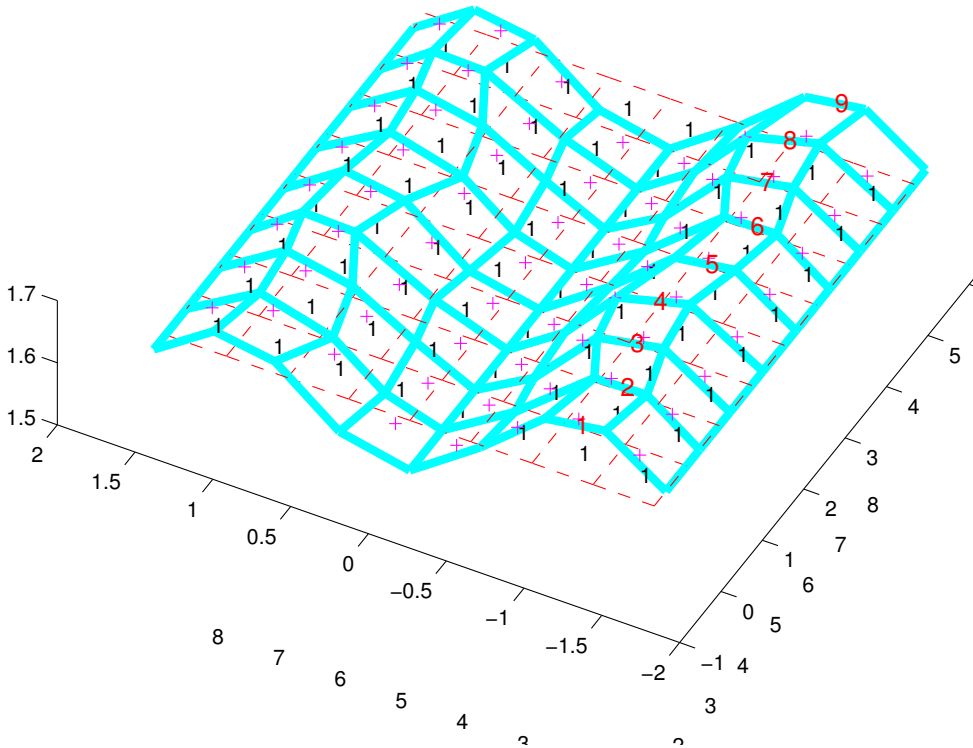

SLICE-3D (cont.)

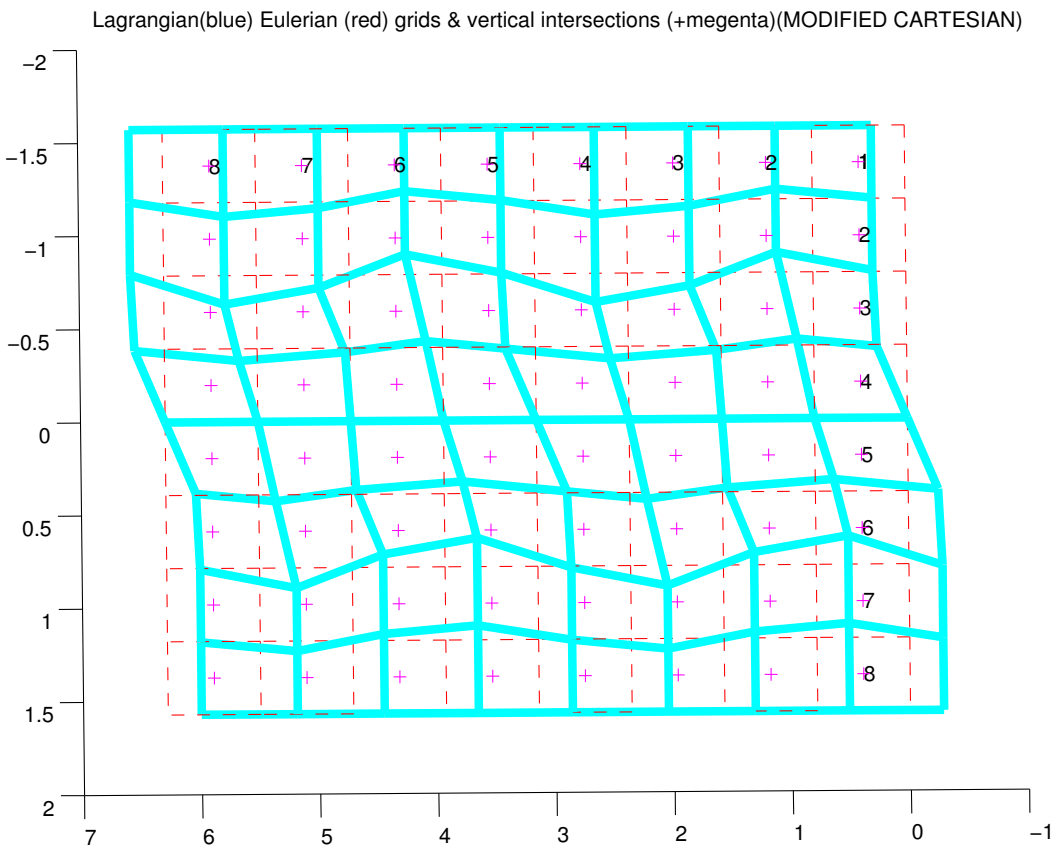

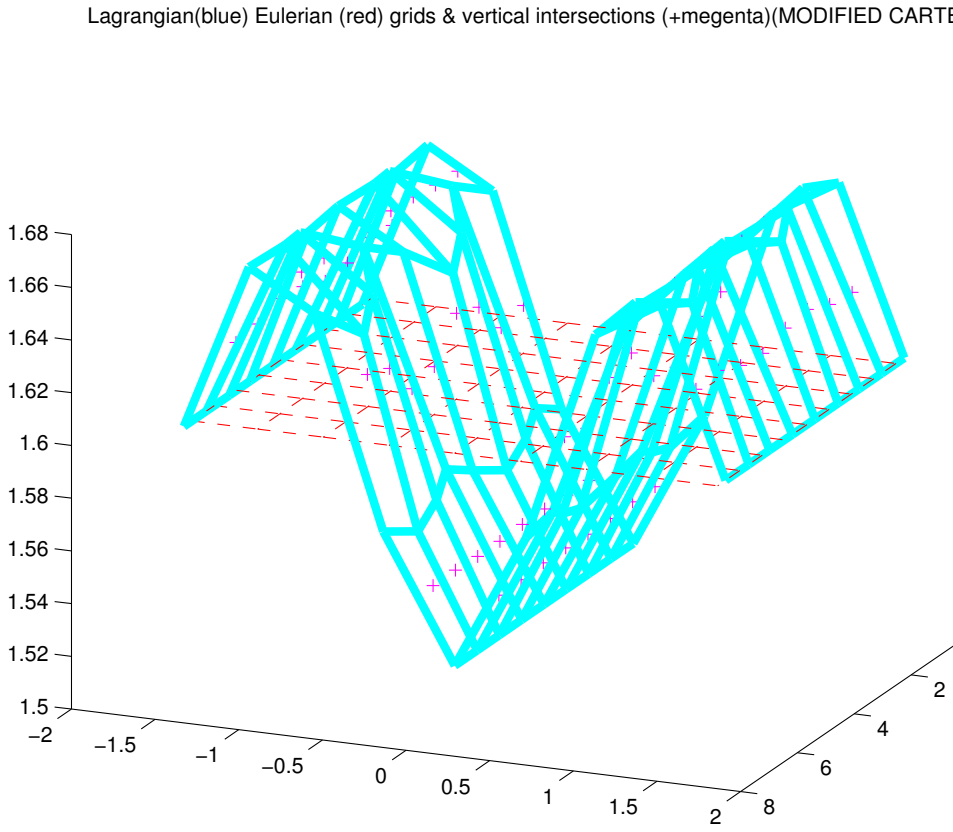

SLICE-3D (cont.)

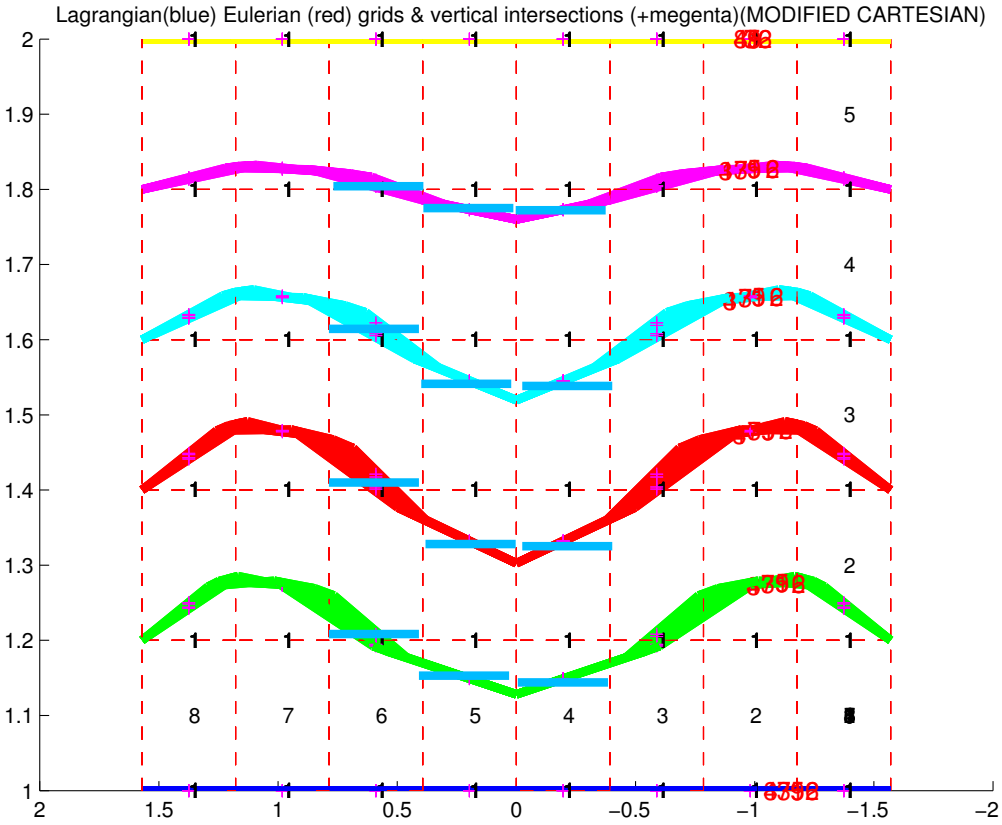

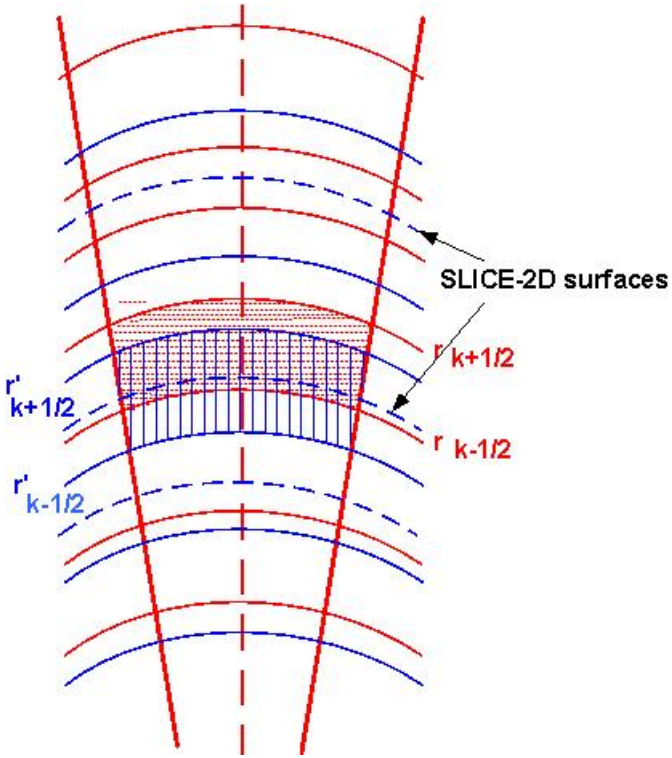

SLICE-3D (cont.)

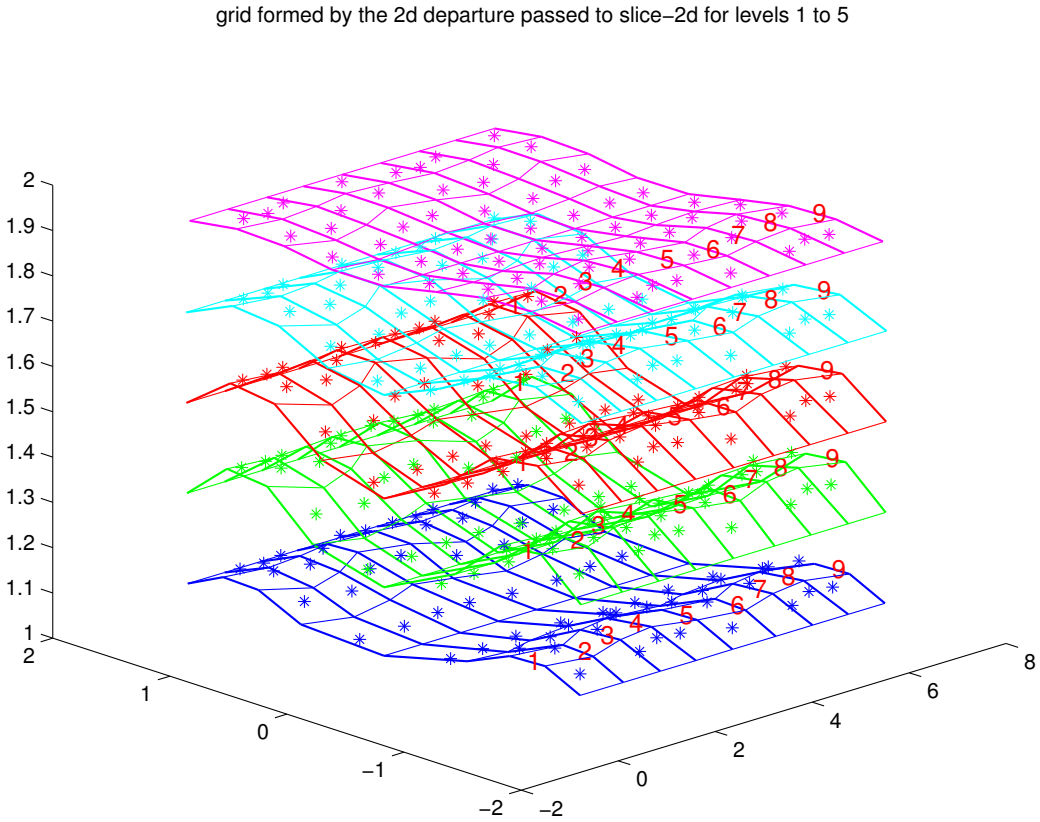

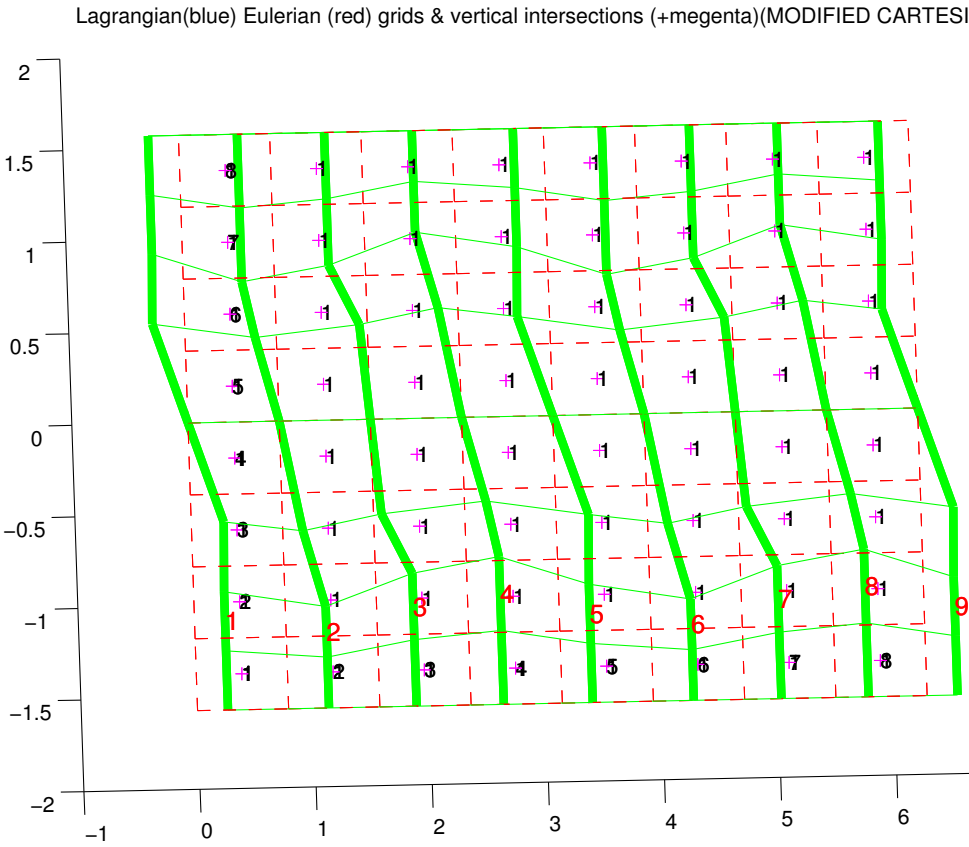

SLICE-3D Intesections

1. Computation of intersections of the spherical shells with the vertical columns. This invloves computing the height (r) at which each deformed spherical shell intersects each vertical column using a bi-linear interpolation. These are needed for vertical remapping.
2. Intersections in the SLICE-2D are intersections of great circles with latitudes circles. These are needed for the second and third cascade remappings.
3. These extra computations are geometry dependent. These are done only once per time step irrespective of the number of scalars. Therefore, this extra cost can be offset by increasing the number of scalars.

Test Problems (A Hadley cell circulation test)

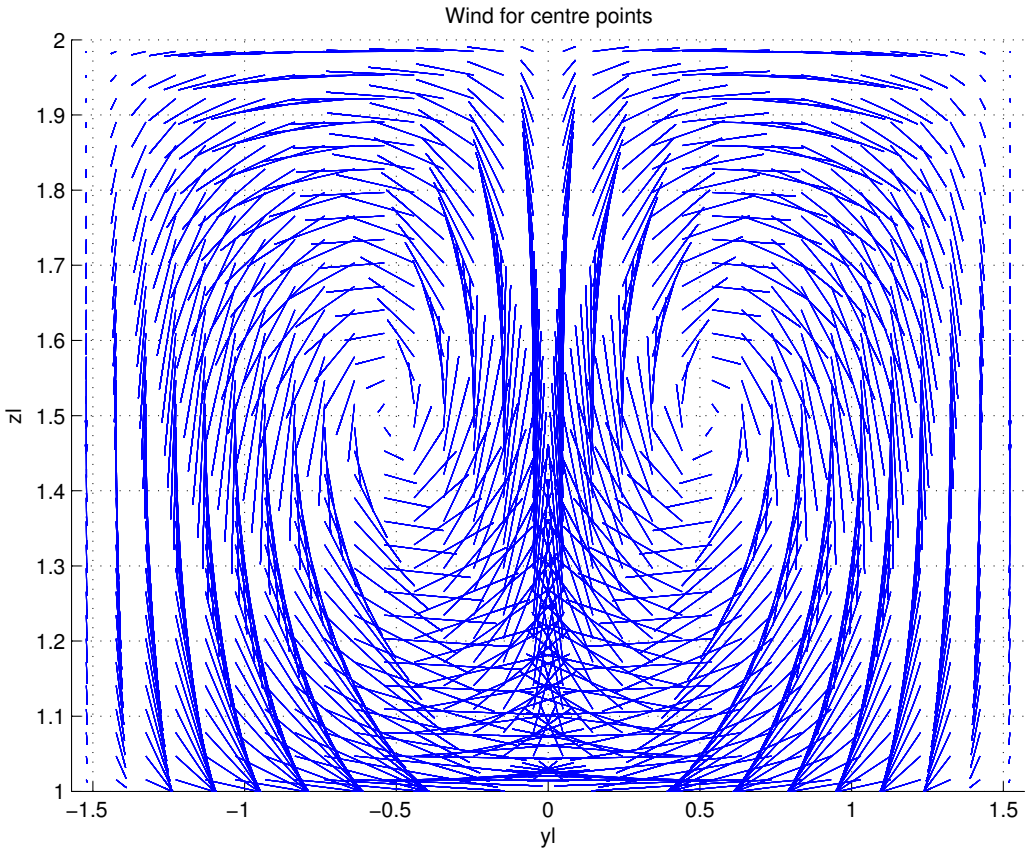

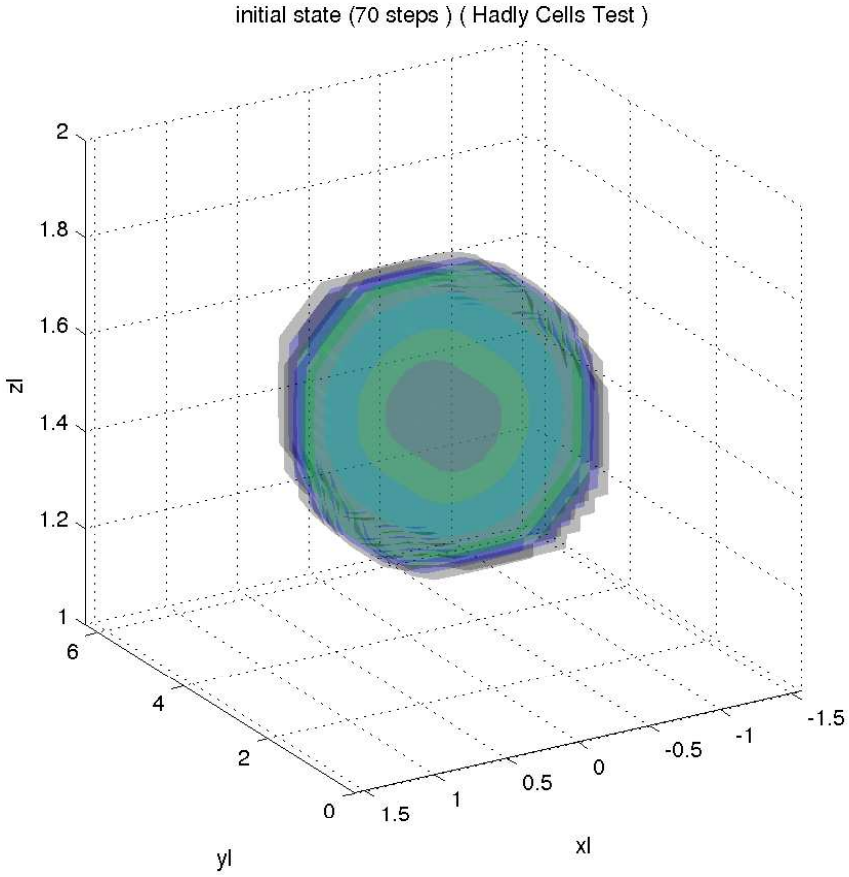

Test Problems (Hadley cells circulation test)

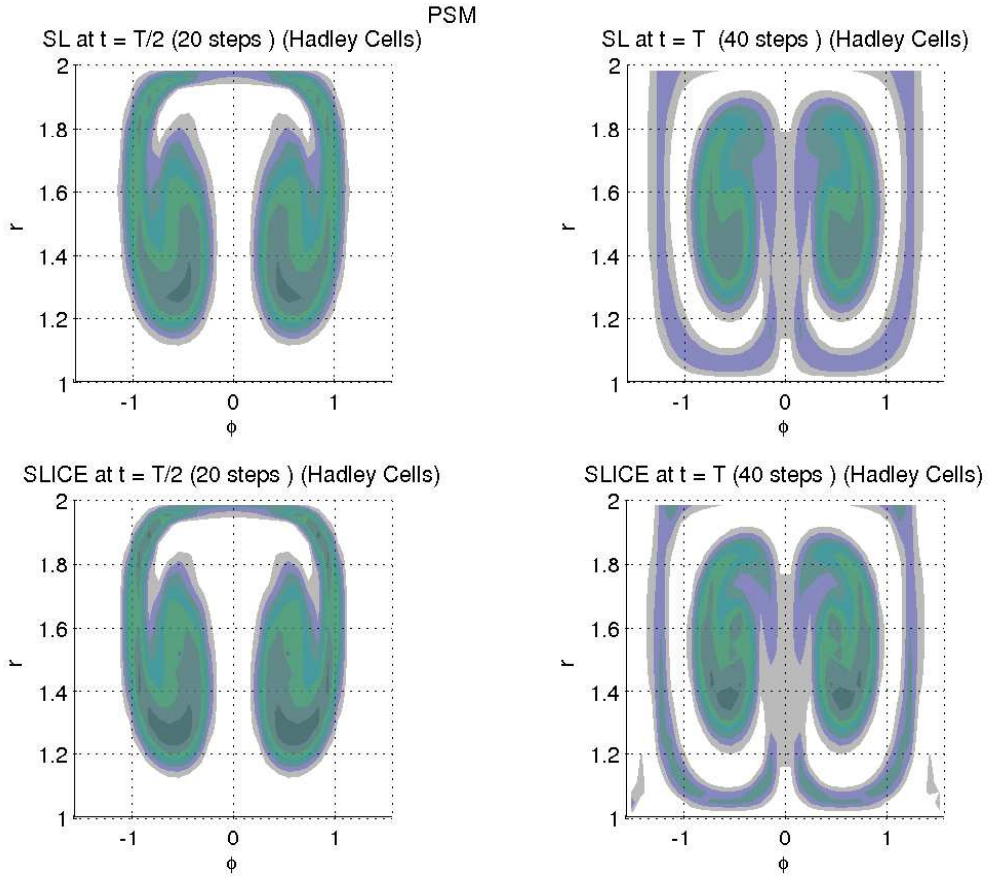

Test Problems (Hadley cells circulation test)

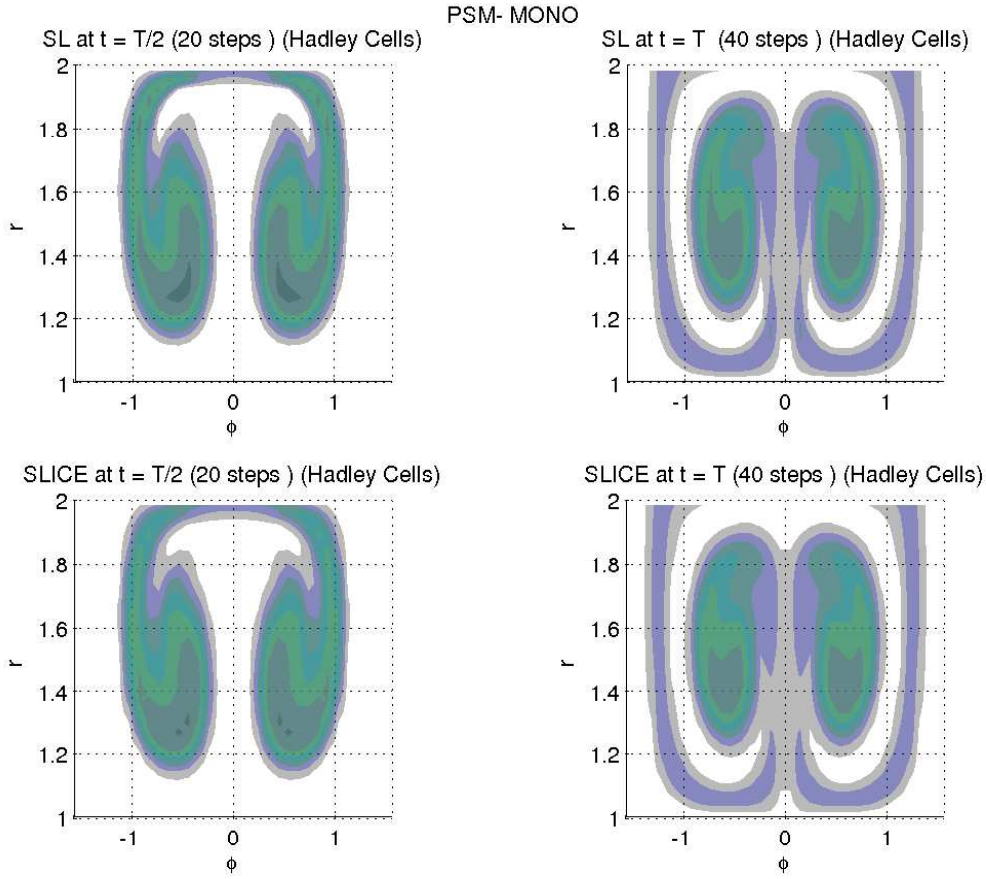

Test Problems (A Rossby wave test)

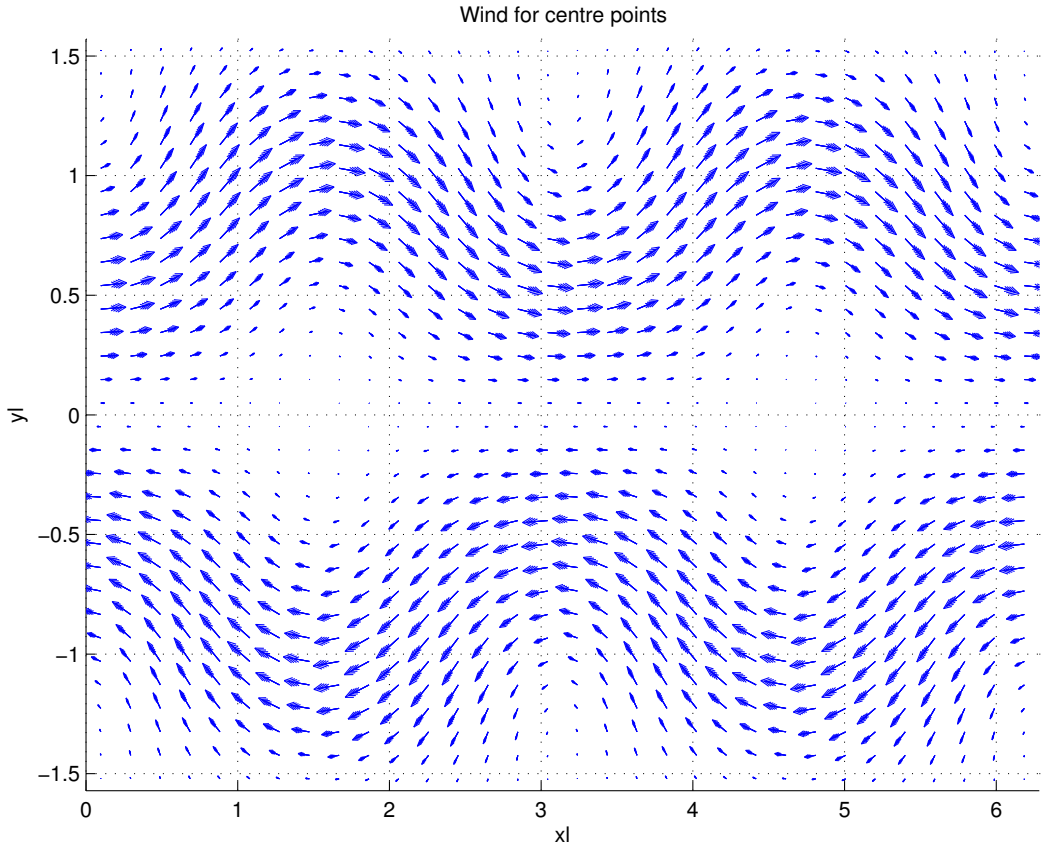

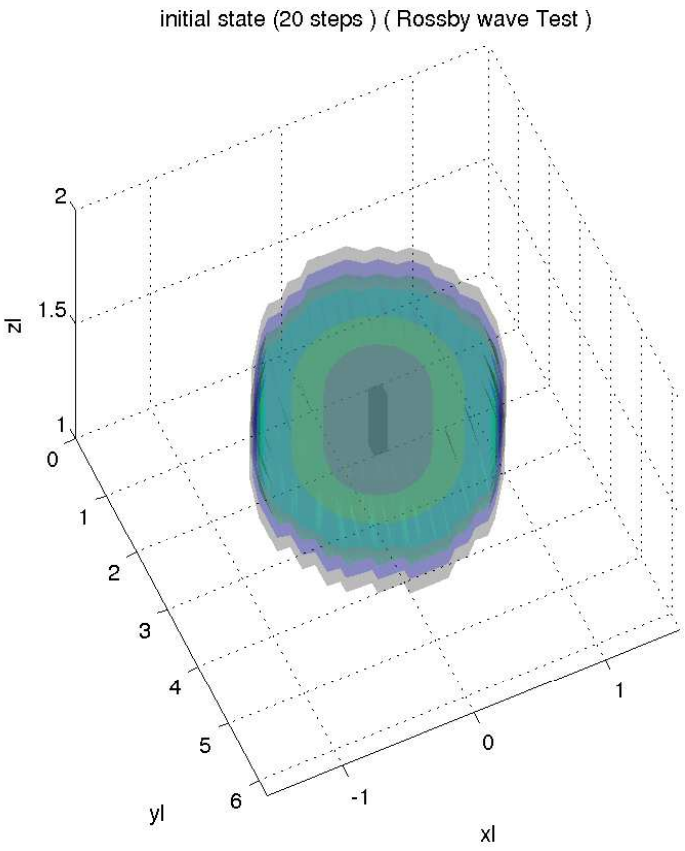

Test Problems (A Rossby wave test)

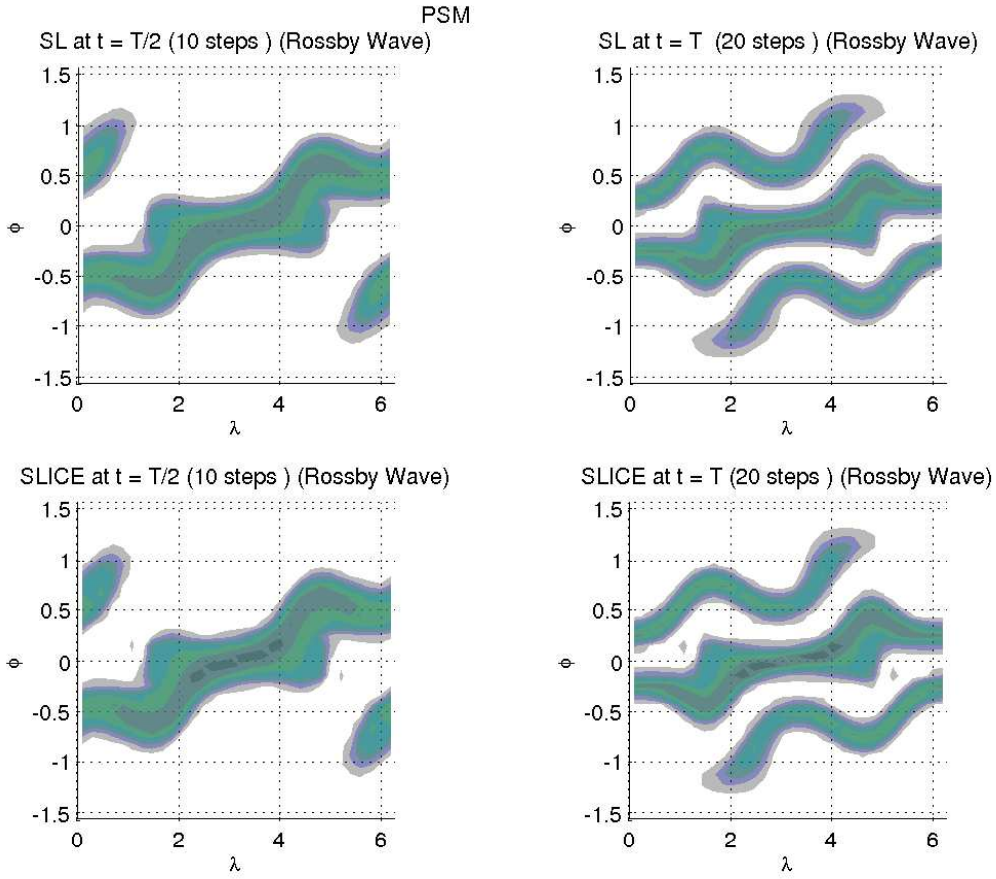

Test Problems (A Rossby wave test)

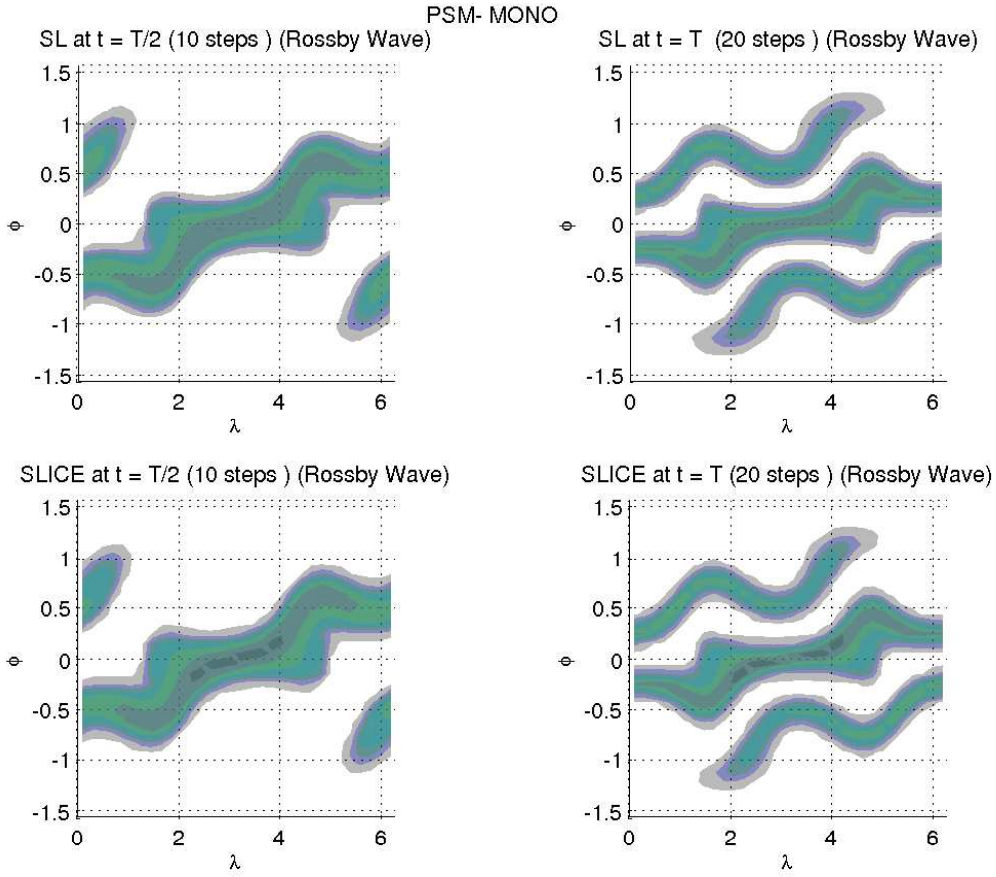

Test Problems (superposed Rossby and Hadley tests)

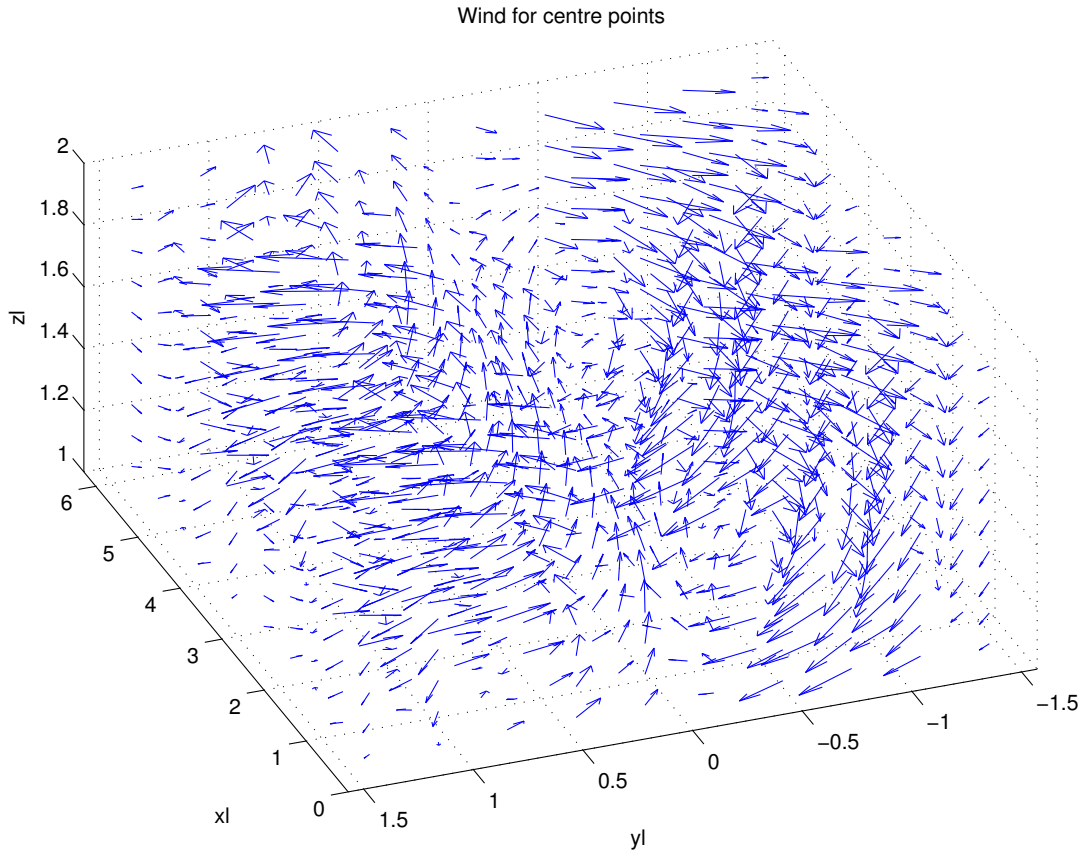

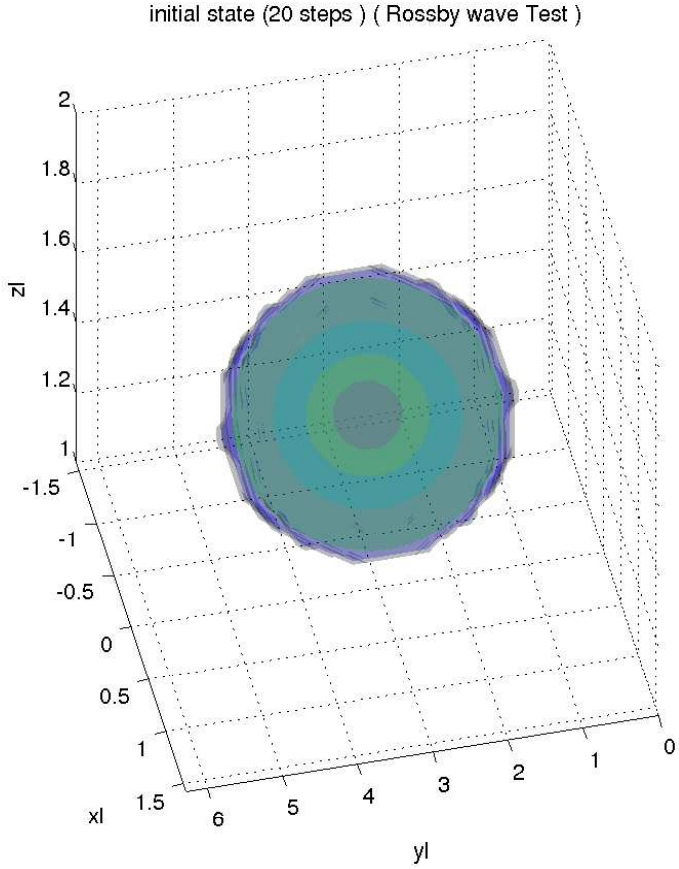

Test Problems (superposed Rossby and Hadley tests)

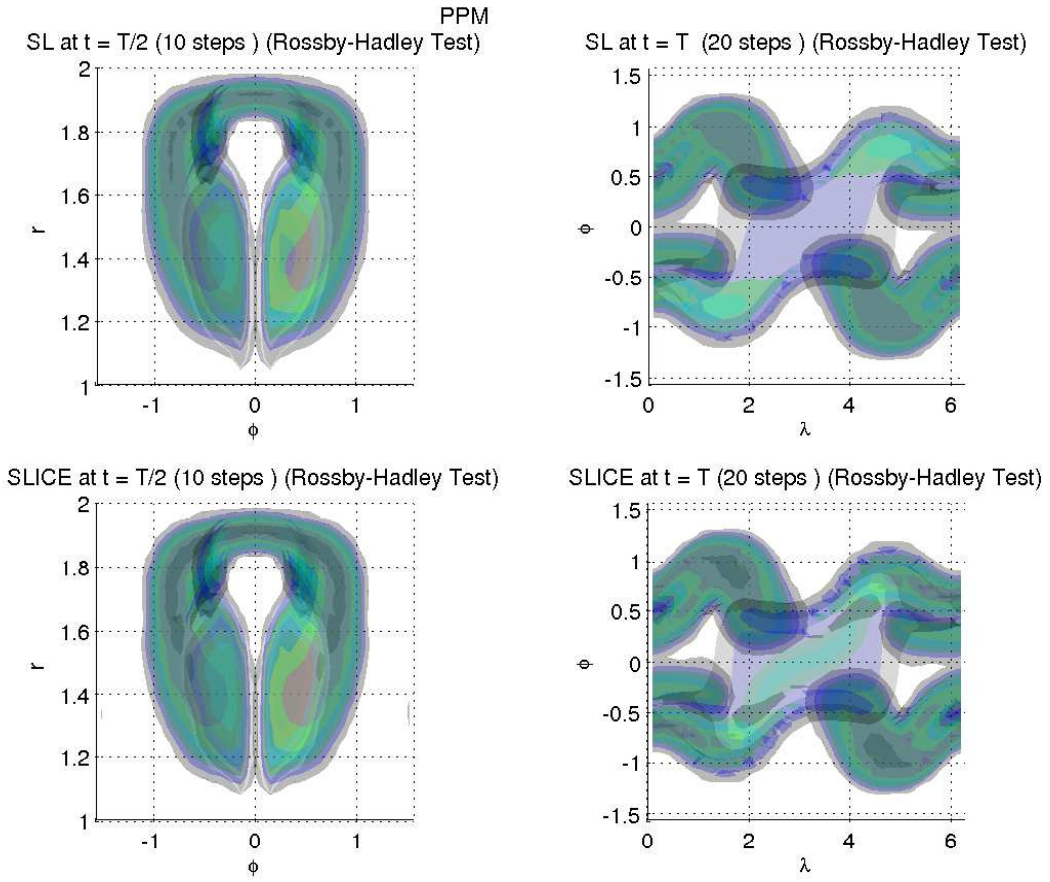

Test Problems (superposed Rossby and Hadley tests)

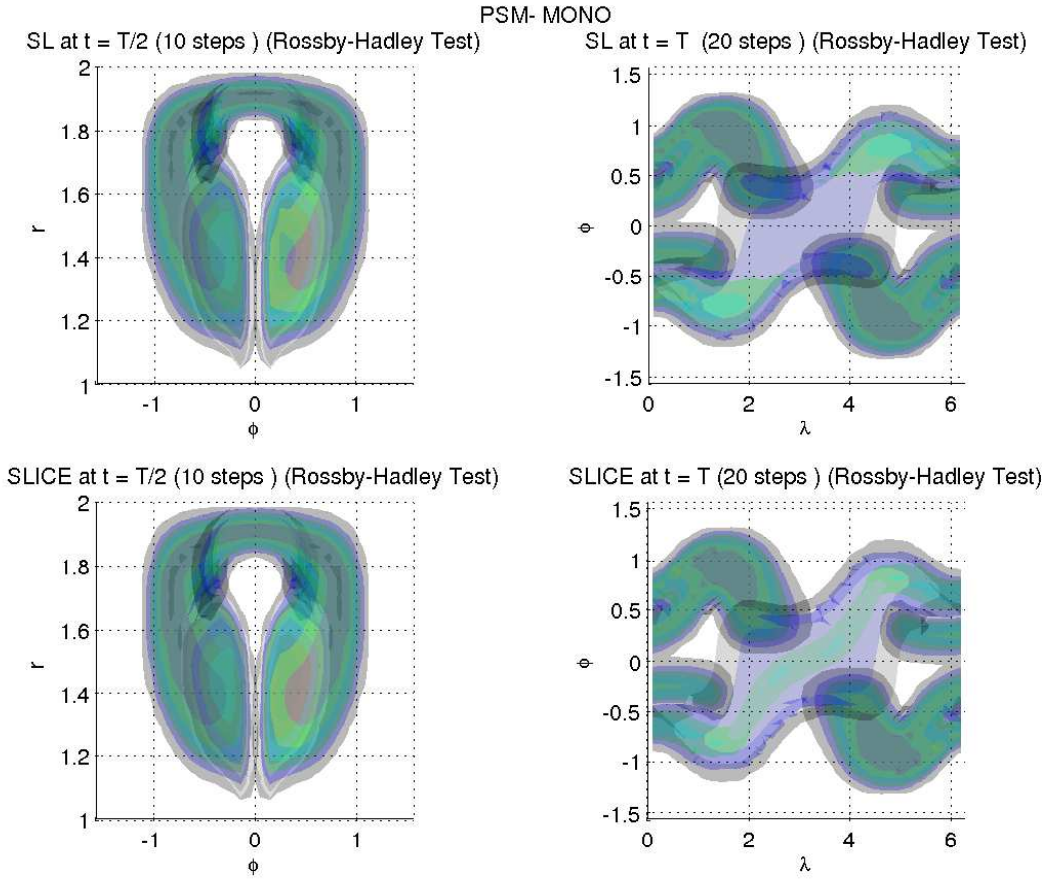

Test Problems (superposed Rossby and Hadley tests)

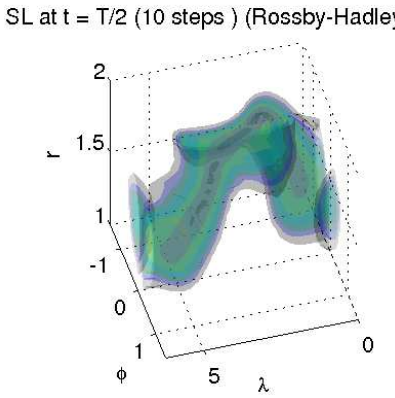

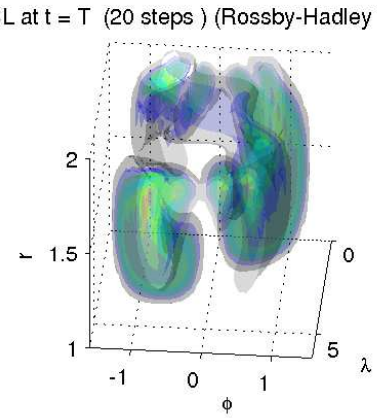

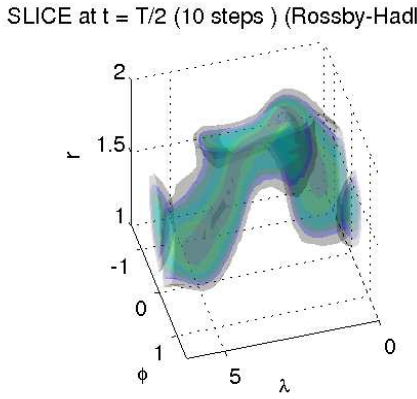

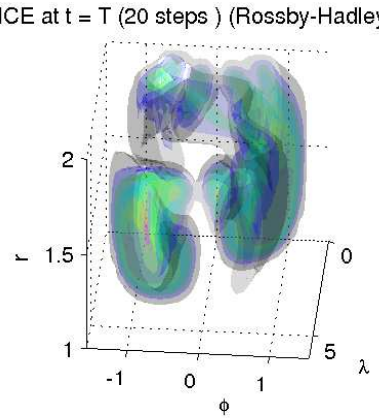

Test Problems (rotated superposed waves)

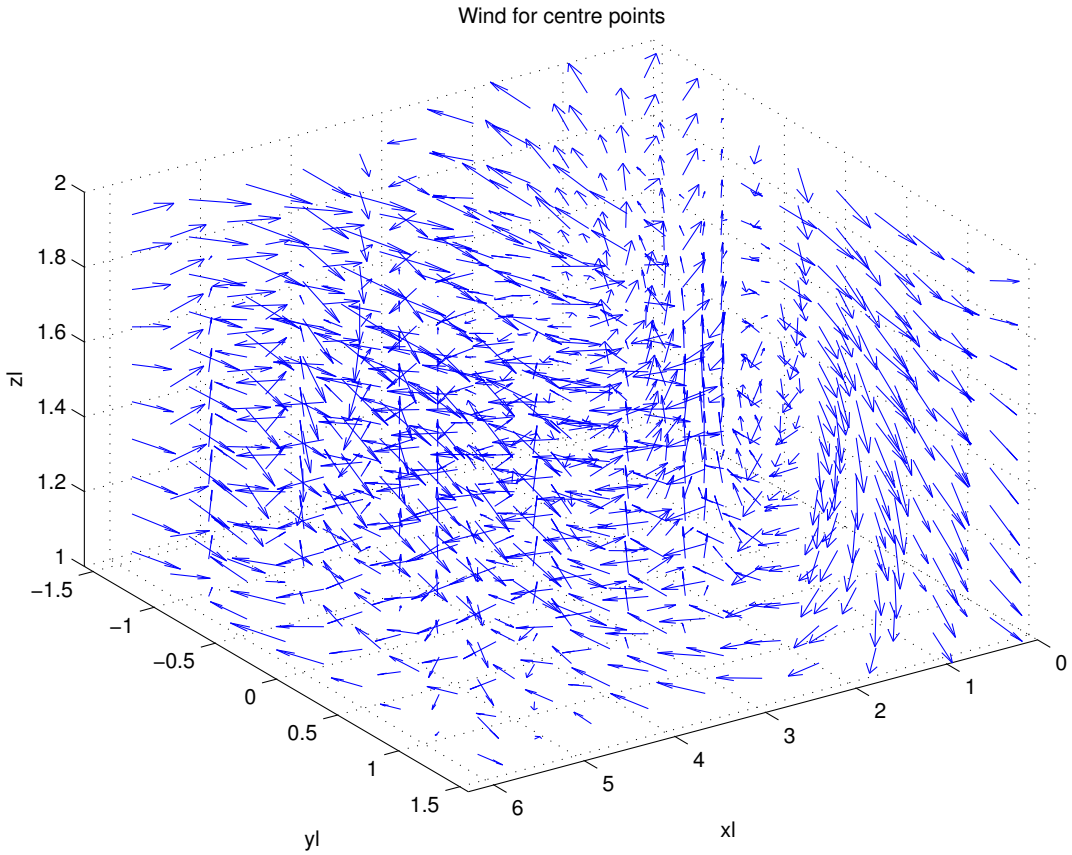

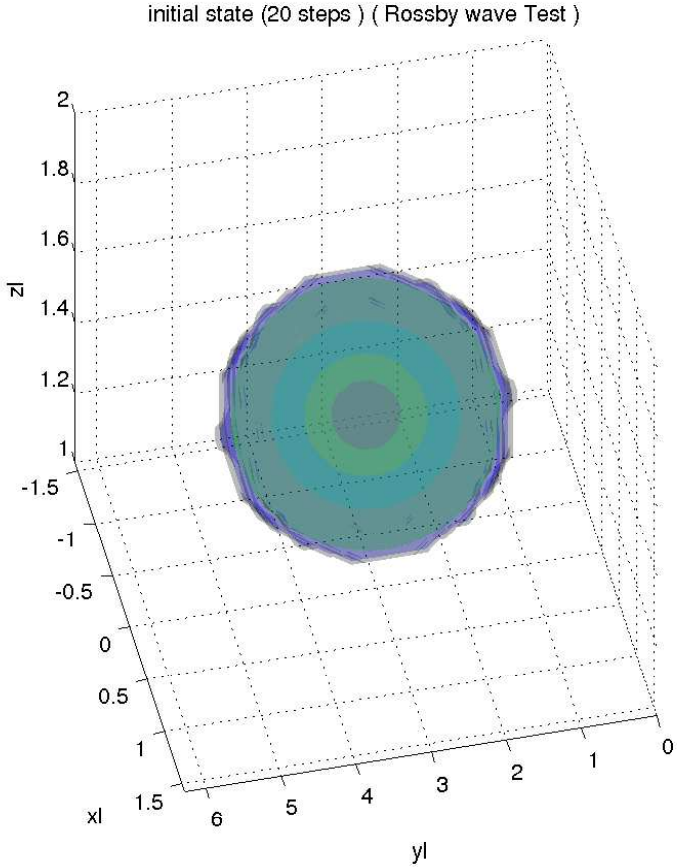

Test Problems (rotated superposed waves)

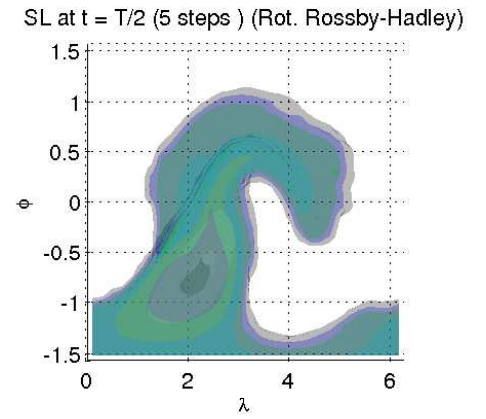

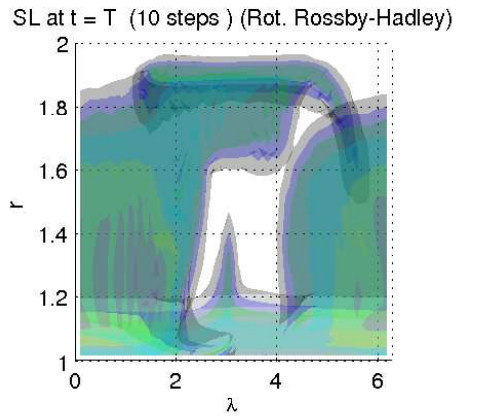

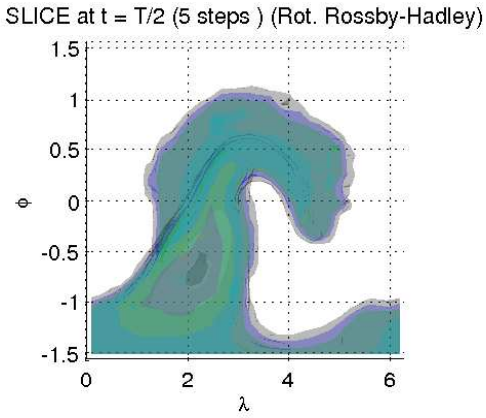

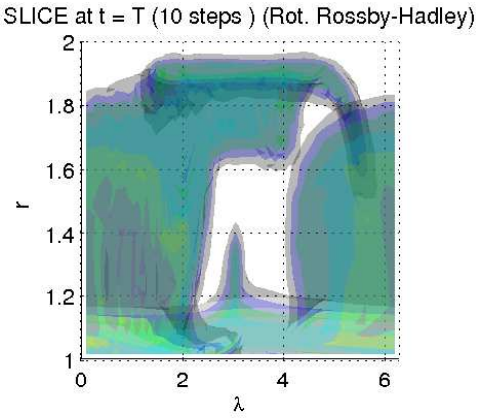

Conclusions

1. **SLICE-3D has been tested on a number of idealised tests and the results show that the scheme is more accurate and efficent compared to tri-cubic interpolating non-conservative SL.**
2. **The scheme (code) is now beeing optimised, implemented, and tested within the UM system.**
3. **The scheme will be an integral part of the next UM dynamical core, and likely to be the default transport algorithm for climate, chemistry and other models.**